

# A Hybrid Approach to Fault Detection and Diagnosis in a Diesel Fuel Hydrotreatment Process

Salvatore L., Pires B., Campos M. C. M., and De Souza Jr M. B.

**Abstract**—It is estimated that the total cost of abnormal conditions to US process industries is around \$20 billion dollars in annual losses. The hydrotreatment (HDT) of diesel fuel in petroleum refineries is a conversion process that leads to high profitable economical returns. However, this is a difficult process to control because it is operated continuously, with high hydrogen pressures and it is also subject to disturbances in feed properties and catalyst performance. So, the automatic detection of fault and diagnosis plays an important role in this context. In this work, a hybrid approach based on neural networks together with a pos-processing classification algorithm is used to detect faults in a simulated HDT unit. Nine classes (8 faults and the normal operation) were correctly classified using the proposed approach in a maximum time of 5 minutes, based on on-line data process measurements.

**Keywords**—Fault detection, hydrotreatment, hybrid systems, neural networks.

## I. INTRODUCTION

THE latest progress in process control has brought various benefits for industrial segments and also a very wide range of new variables for control systems. This situation might lead to an information overload, which is quite alarming since human operators manage the industrial plant in a computer-based environment.

Manufacturing plants are a large source of complexity, since multiple sensors and actuators are inherent. Potential sources of faults or abnormal situations can easily be found.

Manuscript received July 28, 2005. This work was supported by Brazilian Research and Projects Financing Agency (FINEP) and PETROBRAS, the Brazilian State Oil Company, by grant No. 2100/04.

Luciana Salvatore is with the Graduate Program in Chemical and Biochemical Process, School of Chemistry, UFRJ (e-mail: luciana\_salvatore@yahoo.com.br).

Bernardo Nunes Pires is a fellow researcher with Escola de Química, UFRJ (e-mail: bnpires@eq.ufrj.br).

Mário M. M. de Campos is a senior automation engineer working in the research and development center of Petrobras, the Brazilian State Oil Company, Petrobras/CENPES, Cidade Universitária, Quadra 7, Ilha do Fundão, 21949-900, Rio de Janeiro, Brazil; (e-mail: mariocampos@petrobras.com.br).

Maurício B. De Souza Jr. (corresponding author) is a professor at the School of Chemistry, CT, Ilha do Fundão, Bloco E – CP 68542, 21.949-900, Rio de Janeiro – RJ, Brazil (phone: +55-21-2562-7636; fax: +55-21-2562-7567; e-mail: mbsj@eq.ufrj.br).

In regard to this scenario, the process fault detection and diagnosis becomes imperative for the current industrial plant operation.

The use of artificial neural networks (ANNs) has become very successful in process fault detection. There are some very important characteristics that suit the ANNs in the fault diagnosis field. Their ability to analyze non-linear processes, noise tolerance and on-line adaptability enable its industrial use. Also good properties held by ANNs are parallel distributed processing, high degree of robustness or fault tolerance due to the distributed representation, and ability to adapt and continue learning to improve performance [1].

Hoskins and Himmelblau [2] have made a pioneering study of the feasibility of using neural networks for fault detection and diagnosis, using a multilayer feedforward analog perception model. Since then different network architectures have been used for the problem of fault diagnosis [3].

Recently, Venkatasubramanian [3]-[5] performed a systematic and comparative study of various diagnostic methods from different perspectives, including neural networks approaches.

## II. HYDROTREATMENT UNIT MODEL AND SIMULATION

### A. Hydrotreatment Unit (HDT)

Hydrotreating process has become very important in petroleum industry, especially in Brazil. The main objective in this refining process is to give a better use to heavier oil fractions. In this process several components – present in the oil feed – react with hydrogen, following a parallel reaction scheme, inside trickle bed reactors. Hydrogen is mixed to oil in a proportion higher than the stoichiometric. The temperature along the beds rises from the inlet to the outlet, depending on the extent of the exothermic reactions. This catalytic process is carried under severe operational conditions (high temperature and pressure), demanding high production costs, for instance, in hydrogen generation. It is important to mention the environmental advantages in terms of pollutants removal. Therefore, any kind of resistance related to HDT has been disappearing as its advantages increases.

A hydrotreating plant is composed by a reaction section – which includes a series of pre-heating furnaces, the reactors, the hydrogen flash system and the make-up compressor for hydrogen – and a stabilization section. In this work, only the

reaction section is focused. Usually, two reactors are employed. The reactors are trickle bed ones as the inflow enters in gaseous and liquid phases, composing a triphasic system together with hydrogen and the catalyst solid bed.

A quench system is used to control the temperature of the reactors. This is achieved with the injection of a  $H_2$  flow in the middle of catalytic beds.

The yield products of this unit are finally directed to stabilization section, where all commercial specifications will be adjusted.

In the present work, the pre-heating and reaction sections are being explored. The flow-chart of this part of the unit can be seen on Figure 1.

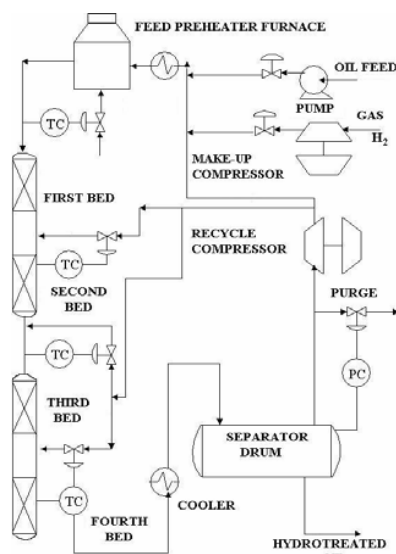


Fig. 1 Reactor and pre-heating section

### B. HDT Unit Modelling

Fixed bed reactors usually show a complex behavior, troubling its control. The difficulties can be summarized as:

- The most important process variable, product concentration is also the most difficult to analyze;
- Inverse response of some dependent variables in relation to variations in the independent variables;
- Dead time associated to thermal wave propagation through the bed;
- Non-linear interaction between kinetic and energetic process;
- Physical-chemical parameters vary in space and time.

In this work, a HDT model developed by Carneiro [6] was selected to represent the real unit and was simulated in MatLab™ and Simulink™ platforms. The modeling equations were chosen in such way that the process shows a similar dynamic to the existing units, by means of concentration and temperature profiles through the catalytic beds. For the furnace and mixer, the model representativity may be relaxed, since these units are accessory and should not demand

computational effort.

In the present investigation, only the first reactor was modeled. The first reactor comprises two beds in series, being designated as first bed and second one. The assumptions of the model for the reactor are:

- Only one reaction occurs and this reaction is 1<sup>st</sup> order with respect to the average concentration of a unique pseudo-reactant A in the pores of the solid phase;
- There is only one fluid phase, with constant physical-chemical properties;
- There is only one solid phase;
- There are no transversal transport phenomena, only longitudinal;
- There is no phase equilibrium;
- The reaction rate is described by the Arrhenius equation;
- There is no variation of volume in the reaction;
- Non-linear interactions between thermal and kinetic processes exist.

The model of the reactor was built assuming that the reactor is composed by  $n$  CSTR-cells (or stages) in series, as previously proposed by Hlaváček [7]. A total of 12 stages were used here. The equations describing this unit were obtained by mass and energy balance in each stage. In the equations described below the mass balances, energy and kinetic model for the HDT unit can be found.

Initially, the flow of mass is described. The fluid phase flows from the left to the right, but back mixtures (in the reverse direction) also happen between successive stages. Then, the flow of the fluid phase between stages is composed by two parcels:  $V_Z$  (direct volumetric flow) and  $g_m$  (volumetric flow associated to reverse flow). It is also assumed that  $g_m$  is constant along the bed and proportional – through adimensional constant  $K_m$  – to  $V_Z$ :

$$g_m = V_Z \cdot K_m \quad (1)$$

The molar flow of component A – where C is the reactant A concentration in fluid phase - is described in the following:

$$\text{Forward direction: } (V_Z + g_m)C = (1 + K_m)V_Z C \quad (2)$$

$$\text{Reverse direction: } g_m \cdot C = K_m \cdot V_Z \cdot C \quad (3)$$

The fluid phase, which is outside the pores of the catalyst, behaves as a perfectly mixed tank, in each stage. The intra-stage mass transfer between solid and gas is based in the external solid catalyst particles surface. The concentration of reactant A inside the pores of the particles ( $C_s$ ) is also considered homogeneous in each stage. The mass flow is proportional to the difference between inside and outside pore particle concentration as shown in equation (4):

$$K_g \cdot a \cdot V(C - C_s) \quad (4)$$

so that  $K_g$  is the mass transport coefficient through the external catalyst particle surface;  $a$  is the external surface area of solid catalyst particles per total stage volume and  $V$  is the total stage volume.

The mass balance for compound A in fluid phase at stage  $i$  can now be written:

$$\{V_Z(1+K_m)C_{i-1} + V_Z \cdot K_m \cdot C_{i+1}\} - \{(2K_m + 1)V_Z \cdot C_i + K_g \cdot a \cdot V(C_i - C_{is})\} = \left\{vV \frac{dC_i}{dt}\right\} \quad (5)$$

where the symbols in the equation above can be described as follows:  $v$  is the interparticle porosity;  $C_{i-1}$  is the concentration in previous stage;  $C_{i+1}$  is the concentration in next stage;  $C_i$  is the concentration in stage  $i$ ;  $C_{is}$  is the concentration in the inner catalyst pore.

The mass balance in solid region at stage  $i$  is given by:

$$\{K_g \cdot a \cdot V(C_i - C_{is})\} = \left\{V(1-v) \frac{dC_{is}}{dt}\right\} + \left\{V(1-v)k_0 \cdot C_{is} \cdot e^{\frac{-E}{R \cdot T_{is}}}\right\} \quad (6)$$

where:  $k_0$  is the Arrhenius kinetic constant;  $E$  is the activation energy;  $R$  is the universal gas constant and  $T_{is}$  is the absolute solid temperature.

For the heat transport,  $g_t$  is the flow of fluid associated to the reverse flow of heat, so that  $g_t$  is also proportional – through adimensional constant  $K_h$  – to  $V_Z$ :

$$g_t = V_Z \cdot K_h \quad (7)$$

The expressions for heat transfer rate intra-stage are given by Equation 8 – in the forward direction – and 9 – in the reverse direction, respectively.

$$(V_Z + g_t) \cdot \rho \cdot C_p \cdot (T_e - T_e^*) = (1 + K_h) V_Z \cdot \rho \cdot C_p \cdot (T_e - T_e^*) \quad (8)$$

$$g_t \cdot \rho \cdot C_p \cdot (T_e - T_e^*) = K_h \cdot V_Z \cdot \rho \cdot C_p \cdot T_e \quad (9)$$

where:  $\rho$  is the gas specific mass;  $C_p$  is the gas specific heat;  $T_e$  is the fluid temperature;  $T_e^*$  is the reference temperature for heat transfer enthalpy calculation

The heat transfer mechanism intra-stage uses a global heat transfer coefficient  $U$  between flow phase and catalyst, based in the external particle surfaces. It is also assumed that the fluid in the catalyst pores is at the same temperature than the solid, as shown in Equation (10) below:

$$U \cdot a \cdot V(T_{es} - T_e) \quad (10)$$

where  $T_{es}$  is the fluid temperature in the bed;  $T_{e,i-1}$  is the fluid temperature in the previous stage;  $T_{e,i+1}$  is the fluid

temperature in the next stage;  $T_{e,i}$  is the fluid temperature in stage  $i$ .

The energy balance in fluid phase at stage  $i$  is described by:

$$\{V_Z(1+K_h) \cdot \rho \cdot C_p \cdot T_{e,i-1} + V_Z \cdot K_h \cdot \rho \cdot C_p \cdot T_{e,i+1} + U \cdot a \cdot V(T_{es} - T_{e,i})\} + \{-(2K_h + 1)V_Z \cdot \rho \cdot C_p \cdot T_{e,i}\} = \left\{v \cdot V \cdot \rho \cdot C_p \cdot \frac{dT_{e,i}}{dt}\right\} \quad (11)$$

The energy balance in solid region at stage  $i$  is presented in the following:

$$\left\{U \cdot a \cdot V(T_{e,i} - T_{is})\right\} + \left\{(-\Delta H_r) V(1-v) k_0 \cdot C_{is} \cdot e^{\frac{-E}{R \cdot T_{is}}}\right\} = \left\{V(1-v) \rho_s \cdot C_{ps} \cdot \frac{dT_{is}}{dt}\right\} \quad (12)$$

The reaction rate  $r_A$  is described by the following kinetic model:

$$r_A = k_0 \cdot C_{is} \cdot e^{\frac{-E}{R \cdot T_{is}}} \quad (13)$$

The furnace modeling consisted solely in the use of an empirical equation of energetic balance. The mixer located in the first bed was modeled with a mass balance generating only one equation.

There are 48 equations described for the first bed, 1 for the mixer, 1 for the furnace and 48 for the second bed. A simulation algorithm was developed to represent the model and was implemented in Simulink™.

The simulation parameters were maintained according to the Simulink™ default, adjusting the integration method to ode15s, able to solve stiff algebraic-differential equations. The simulation time was of 25000 seconds for all points tested.

The process exhibited inverse response and time delay. Two PI (Proportional-Integral) controllers were tuned by the Internal Model Control method [8], one to control the outlet temperature of the furnace, manipulating the flow of fuel to be burned, and another to control the outlet temperature of the second bed, manipulating the hydrogen quench flow to the mixer. It was assumed for the closed loop experiments that there are no instrumental errors and that there is no noise in the instruments.

### III. FAULT ANALYSIS

For the generation and analysis of faults in this process, two input variable of the system were chosen to be disturbed: the inlet feed concentration and the inlet flow rate. The normal process operational range for reactant concentration is 17-22 mol/m<sup>3</sup> and between 0.07-0.1 m<sup>3</sup>/h for the inlet flow.

From these values of concentration and flow, the conditions of abnormal situation for the system were established. These ranges and combination of values for concentration and flow

are described on Table I.

TABLE I  
PROCESS CONDITIONS TESTED

Condition	Feed concentration (mol/m <sup>3</sup> )	Feed flow (m <sup>3</sup> /h)
1	22	0.1
2	17	0.1
3	22	0.07
4	17	0.07
5	24.5	0.115
6	24.5	0.055
7	14.5	0.115
8	14.5	0.055
9	24.5	0.1
10	14.5	0.1
11	22	0.055
12	22	0.115
13	17	0.055
14	17	0.115
15	24.5	0.07
16	14.5	0.07

After disturbances, the following process responses were analysed:

- Furnace outlet temperature;
- Outlet reactor 1 temperature;
- Outlet reactor 1 concentration;
- Hydrogen quench flow in the mixer;
- Outlet concentration of the mixer;
- Outlet temperature of the mixer;
- Outlet temperature of reactor 2;
- Outlet concentration of reactor 2.

#### IV. NEURAL NETWORK STRUCTURE

MLP (Multilayer Perceptron) and RBF (Radial Basis Function) [9] networks were used. The following variables, generated in the previous step, were chosen as input ones, where  $k$  is the sampling time:  $T1(k)$  and  $T1(k-1)$  - outlet reactor 1 temperature,  $T2(k)$  and  $T2(k-1)$  - outlet temperature of reactor 2,  $(dT2/dt)(k)$  - outlet temperature derivative of reactor 2,  $H2(k)$  - Hydrogen quench flow in the mixer and  $CARGA(K)$  - inlet feed concentration.

The conditions described in Table I were divided in nine classes of faults and defined as the output to the network, as follows in Table II:

TABLE II  
CLASSES OF FAULTS

Conditions	Fault	Process situation
1, 2, 3, 4	0	Normal
9, 15	1	High Concentration
10, 16	2	Low Concentration
11, 13	3	Low Flow
12, 14	4	High Flow
5	14	High Concentration and Flow
6	13	Low Concentration and Flow
7	24	Low Concentration and High Flow
8	23	Low Concentration and Low Flow

All neural network methodology, including training and validation were carried out in Statistica™ 6.0 software.

For a better comparison, another procedure was tested. Three networks were trained to become specialized in a group of classes. The faults cases were separated according to the logic showed in Figure 2.

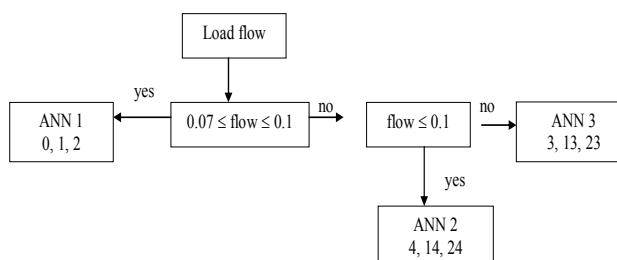


Fig. 2 Separated network approach flow-chart

#### V. THE POS-TREATMENT ALGORITHM

In this section, it is proposed a MatLab™ algorithm called WINNER in order to show to the operator the classification of an abnormal event. The steps followed were:

- The network generates data in a period of 1 second;
- At each 2,5 minutes, 150 classifications are checked.

A winning class will be found if the net achieves at least the best performance percentage during classification. This means that this algorithm searches the number of times when the same class was identified. In this case, the system informs the winning class. If that percentage is not reached the net renders a NK ("not known") status.

#### VI. RESULTS

##### A. Faults Generation in Simulink™

Figures 3 to 5 show, respectively, the results of variations in the temperature of first and second beds and flow of hydrogen response with time in normal and abnormal conditions. These results are showed accordingly to the class faults separation described earlier. It must be noticed that only the first 900 seconds were shown because it is our purpose to detect the faults in an interval of minutes. The curves in the

first graphic in the left, show the responses corresponding to normal operation, while the other curves show the classes of abnormal operation, separately.

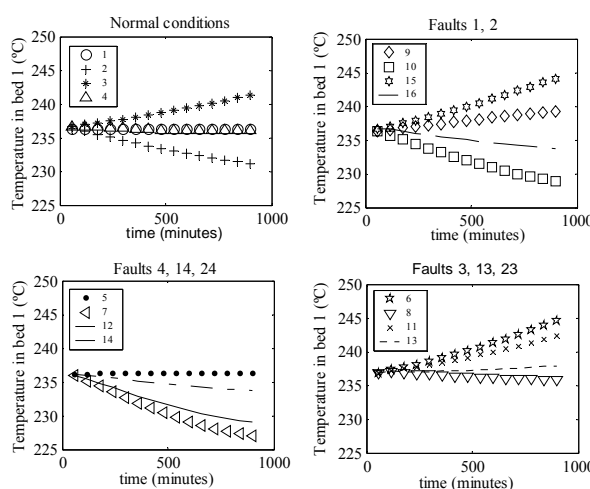


Fig.3 Temperature responses in the first bed

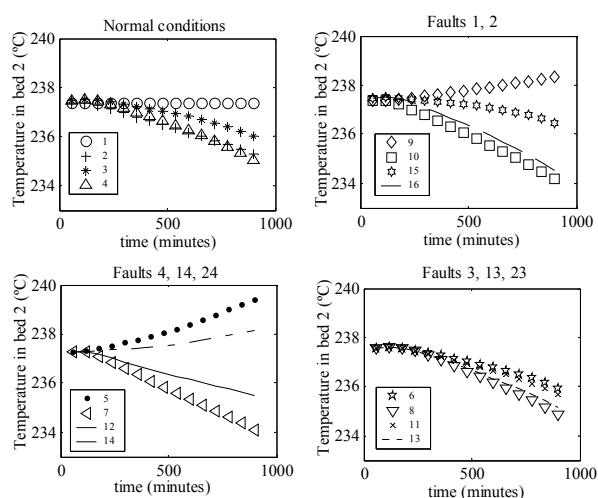


Fig. 4 Temperature responses in the second bed

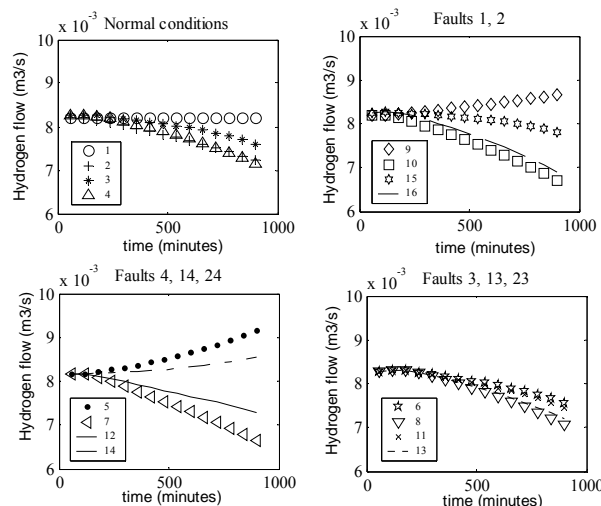


Fig. 5 Hydrogen quench flow response

### B. Neural Network Results

Table III shows the final networks obtained in both strategies (one single network and three networks).

TABLE III NEURAL NETWORKS OBTAINED			
Network type		Training performance	Selection performance
1 network	RBF	97%	96%
3 networks	RBF	97%	96%
tested	RBF	98%	98%
	RBF	97%	97%

### C. Post-Treatment Results

After neural network training and validation a prediction analysis was carried out in order to compare and evaluate the time required by the detection system to inform the fault status to the operator.

As all networks showed at least a 96% performance, when the WINNER program verified 144 equal classifications, it was said that a class was recognized.

Table IV shows the comparison between the each neural network ensemble. It can be seen how long, in minutes, each net takes to send the error signal to the operator.

TABLE IV  
NEURAL NETWORKS DETECTION PERFORMANCES

Fault	Stand-alone Net	Ensemble		
		Net 1	Net 2	Net 3
0	2,5	2,5	-	-
1	5	5	-	-
2	5	5	-	-
3	2,5	-	-	2,5
4	5	-	5	-
14	5	-	5	-
13	5	-	-	5
24	5	-	5	-
23	5	-	-	5

For the approach using only one neural network, the tests presented 100% performance when in the normal process operation range, sending after 2.5 minutes a fault signal to the operator. For the disturbances cases, this time turned to 5 minutes.

For the other methodology, where three specialized neural networks were used, net 1 took 5 minutes to recognize faults 1 and 2 (2,5 minutes to identify normal operation), net 2 took 5 minutes for all faults and net 3 took 5 minutes for faults 13 and 23 (2,5 minutes for fault 3).

## VII. CONCLUSIONS

The two approaches tested for conjunction of neural networks with a post-processing classification algorithm resulted in very efficient hybrid systems for fault detection of the HDT unit. In 5 minutes both approaches were able to correctly classify the fault classes. However, the approach that considers multiple networks might work better in a case where more faults are present.

In the continuation of this work it is intended to simulate the section of hydrogen compression and to extend the fault diagnosis system in order to include the disturbances associated with that section.

## REFERENCES

- [1] R. P. Lippmann, "An introduction to computing with neural nets." *IEEE ASSP Mag* 4, pp. 4-22, 1987.
- [2] J. C. Hoskins, D. M. Himmelblau, "Artificial neural network models of knowledge representation in chemical engineering" *Computers and Chemical Engineering*, vol. 12., pp. 881-890, March 1988.
- [3] V. Venkatasubramanian, R. Renghunanathan, S. N. Kavuri, K. Yin, "A review of process fault detection and diagnosis Part III: Process history based methods" *Computers and Chemical Engineering*, vol. 27, pp. 327-346., April 2002.
- [4] V. Venkatasubramanian, R. Renghunanathan, S. N. Kavuri, K. Yin, "A review of process fault detection and diagnosis Part I: Quantitative model- based methods" *Computers and Chemical Engineering*, vol. 27, pp. 293-311, April 2003.
- [5] V. Venkatasubramanian, R. Renghunanathan, S. N. Kavuri, K. Yin, "A review of process fault detection and diagnosis Part II: Qualitative models and search strategies" *Computers and Chemical Engineering*, vol. 27., pp. 313-326, April 2003
- [6] H. L. Pinheiro, "Controle robusto de reator químico de leito fixo" M.S. thesis, COPPE, UFRJ, Rio de Janeiro, Brazil, 1992.
- [7] V. Hlavacék, "Fixed bed reactors, flow and chemical reaction residence time distribution theory in chemical engineering", (Petho, Arpad, Richard D. Noble, eds, Verlag Chemie, Weinheim, 1982, pp.103-111
- [8] M. Morari, E. Zafiriou, "Robust process control", Prentice Hall, Englewood Cliffs, New Jersey, U.S.A., 1989.
- [9] S. Haykin, "Neural networks – A comprehensive foundation", 2nd edition, Ed. Prentice Hall, 1999.